Laser ablation of polylactic acid sheets for the rapid prototyping of sustainable, single-use, disposable medical micro-components

Laser ablation of polylactic acid sheets for the rapid prototyping of sustainable, single-use, disposable medical micro-components

Alfredo E. Ongaro[1,2,3], Ieva Keraite [1,2], Antonio Liga[1,2], Gioacchino Conoscenti[3], Stuart Coles[4], Holger Schulze[2], Till T. Bachmann[2], Khaled Parvez[5], Cinzia Casiraghi[5], Nicola Howarth[1], Vincenzo La Carubba[3,6] & Maïwenn Kersaudy-Kerhoas[1,2]*

[1] Institute of Biological Chemistry, Biophysics and Bioengineering, School of Engineering and Physical Science, Heriot-Watt University, Edinburgh EH14 4AS, United Kingdom

[2] Division of Infection and Pathway Medicine, Edinburgh Medical School, College of Medicine and Veterinary Medicine, The University of Edinburgh, Edinburgh EH164SB, United Kingdom

[3] Department of Civil, Environmental, Aerospace and Materials Engineering (DICAM), University of Palermo, Viale delle Scienze building 6, 90128 Palermo, Italy

[4] Sustainable Materials and Manufacturing Group, WMG, University of Warwick, Coventry, CV4 7AL, United Kingdom

[5] School of Chemistry, University of Manchester, Manchester M13 9PL, United Kingdom

[6]ATeN Center – CHAB, Università di Palermo, Viale delle Scienze building 18, 90128 Palermo, Italy

*e-mail: M.Kersaudy-Kerhoas@hw.ac.uk

ABSTRACT: The employment of single-use, disposable medical equipment has increased the amount of medical waste produced and the advent of point-of-care diagnostics in lab-on-chip format is likely to add further volume. Current materials used for the manufacture of these devices are derived from petroleum sources and are, therefore, unsustainable. In addition, disposal of these plastics necessitates combustion to reduce infection risk, which has, depending on material composition, an undesirable environmental impact. To address these issues, we have developed a general approach for the rapid prototyping of single-use point-of-care cartridges prepared from polylactic acid, a sustainable material which can be milled, laser-cut as well as moulded for translation to mass-market products. Here, the laser workability of polylactic acid sheets is reported together with examples of microfluidic components. Furthermore, the low molecular adsorption in laser-ablated polylactic acid channels and the compatibility of polylactic acid for common on-chip bioassays, such as polymerase chain reaction (PCR), are demonstrated. This innovative prototyping technique can be easily translated to high volume manufacturing and presents exciting opportunities for future sustainable microfluidic laboratories as well as potential for sustainable disposable single- use microcomponents for clinical applications.

KEYWORDS: Polylactic acid; Polymethylmethacrylate, CO_2 laser cut; Sacrificial Layer Assisted Manufacturing; kerf; Point of care; micromachining; microfluidic; layer by layer; rapid prototyping

INTRODUCTION The demand for point-of-care testing is increasing at a fast pace and the majority of these new tests are likely to be carried out in disposable plastic chips in order to eliminate the possibility of cross-contamination and alleviate the need for time-consuming sterilisation. However, despite this clear trend[1] and the fact that plastic waste has become a global challenge[2] , there are only a limited number of reports in the literature focusing on the full life cycle of products used in the point-of-care environment[3]. Nearly all commercially available plastic chips or cartridges are made from petroleum-derived materials, these include predominantly polymethylmethacrylate (PMMA), cyclo olefin copolymer (COC), polycarbonate (PC) and polystyrene (PS). These non-degradable polymers are currently favoured for the production of microfluidic devices by both academic laboratories and industry and mirror the traditional plastic medical waste routes. Similarly, there is not enough debate about the amount of waste that disposable point-of-care devices will generate or how to deal with this type of waste, whether in a hospital or resource-poor setting. It has been shown that inadequately controlled incineration procedures and waste streams lead to the release of significant quantities of pollutants[2,4]. Furthermore, anecdotal evidence gathered in Asia, Africa and South America, indicated that incinerators may not always operate properly or be manned by competent personal.[5,6,7]Thus, the additional waste generated by the increased consumption of disposable medical items may exacerbate these problems for such communities. Replacement of non-degradable polymers with biodegradable alternatives from non-fossil resources could be one solution to the growing concern around the increased production of pollutants from medical plastic waste.[11] A material of interest in this regard is polylactic acid (PLA), a common biodegradable thermoplastic produced from the naturally occurring compound, lactic acid

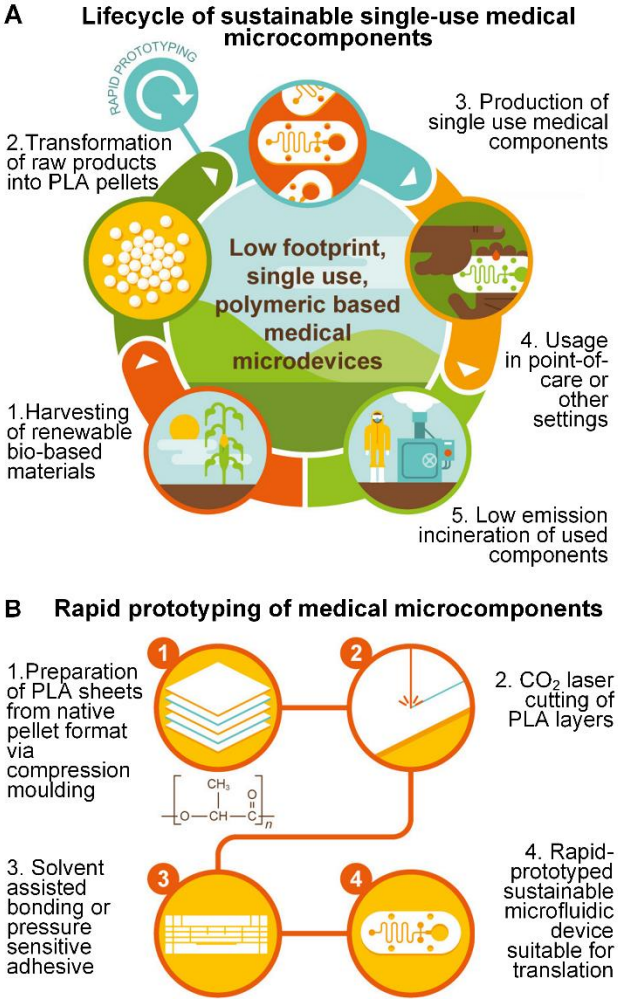

Figure 1. A) Conceptual lifecycle for polylactic acid (PLA) based single-use medical micro-components such as microfluidic chips. From the lower left illustration clockwise: PLA monomers are produced via fermentation of corn or sugar taken from starch plants. The amount of equivalent CO_2 per Kg of PLA Ingeo for the Corn production is about 0.25 kg CO_2 eq./ kg; the transformation from the raw product into PLA pellets is 1.038 kCO_2 eq./ kg PLA naturework ingeo; the production of the microfluidic device from the pellets; usage of the microfluidic component in point-of-care or other settings; Incineration as possible end-of-life scenario of the PLA microfluidic device. Other possible scenarios in function of the application of the device are mechanical recycling (0.6 kg CO_2 eq./ kg), industrial composting (1.5 kg CO_2 eq./ kg), anaerobic digestion (1 kg CO_2 eq./ kg), direct fuel substitution in industrial facility (0.1 kg CO_2 eq./ kg) and incineration with heat recovery (1. kg CO_2 eq./ kg)[8,9,10] Resulting in, at least, half lower impact on the climate change with respect to other thermoplastic material from non-renewable resources. B) Rapid Prototyping scheme for the production of PLA based devices. In inset: chemical structure of PLA.

which itself is prepared from the simultaneous saccharification and fermentation of starch. With good biocompatibility credentials and approved by the US Food and Drug Administration (FDA) for use in humans, PLA has attracted much attention recently being utilised in tissue engineering, medical implants, surgical sutures, packages, fibres and textiles[8] as well as being identified as a potential alternative material for the production of disposable biomedical items. The latter application is further supported by the finding that the impact of waste PLA combustion is significantly lower than that of other plastics.[12] Analogous to the petroleum-derived materials, PLA can be processed to high-volume by extrusion or injection molding.

Having selected a material for the production of sustainable single-use medical microcomponents, we turned our attention to developing a method that would allow the rapid-prototyping of devices. Rapid-prototyping methods have had enormous impact on manufacturing by allowing rapid iterations between design and testing of new product ideas.[13, 14]

Recent advances in additive manufacturing, resolution have permitted prototyping features at a microscale. PLA thanks to its low elasticity and low melting point has become a material of choice for additive manufacturing techniques such as Fused Deposition Modelling[15] (FDM, or commonly referred as 3D printing). A few examples involving the 3D printing of PLA microfluidic chips have been reported.[16] However, 3D printing still poses some challenges which prevents this technique being used routinely for the production of these devices; namely printing time, complexity of multi-material manufacturing, artefact assembly, print fidelity, often necessary post treatments, difficulty in removing supporting material and limited printer resolution (down to 300-500 µm is achievable for minimal feature).[17,18] On the other hand, a layer-by-layer approach enables flexibility in the design, does not require post treatment and can be applied to an unlimited number of materials.[19,20] It also allows for surface and local treatments and for electrodes and membrane integration, for the production of hybrid microfluidic devices. Furthermore, advances in multi-layer rapid-prototyping techniques have permitted the manufacturing of complex microfluidic devices in less than 15 minutes from design to test.[21] This method involves laser cutting individual layers followed by multi-layer bonding using a solvent assisted method.

Here, we propose a design for sustainability (DFS) approach[22] for the production of environmentally friendly medical microcomponents (Figure 1A). In this scheme, PLA is transformed from biomass into pellets. These pellets are transformed into sheets which are used into a rapid-prototyping technique until a final design is put into production and the device is then manufactured via injection moulding, for example. The disposable medical micro-components may be used in clinical settings, home settings or in the field (ambulance, mobile laboratories). Devices in contact with clinical samples such as blood, urine, or sweat are incinerated. In this scheme, several steps are well established. The harvesting of biomass for transformation of raw product into pellets is already commercially viable. Similarly, the high-volume production of PLA components is well controlled. The missing step for researchers and engineers is the ability to rapid-prototype microscale devices prior to production.

We here report the development of a simple and affordable layer-by-layer laser-based technique to engineer complex single-use microfluidic chips from PLA (Figure 1B). No solvent or harsh conditions are employed and the technique only necessitates the use of low capital investment equipment. We demonstrate good PLA workability in conjunction with CO_2 laser cutting and engraving, using a Sacrificial Layer Assisted Manufacturing method (SLAM). Following the observation of very low surface roughness, the potential benefits offered by

integrated PLA-derived fluidic devices are presented through an investigation into molecular retention. Finally, complex microfluidic networks have been produced to show the potential of this technique for the rapid-prototyping of micro-engineered components for biomedical uses, in particular for point-of-care diagnostics.

MATERIALS AND EXPERIMENTAL SESSION

PMMA and PLA material

PMMA was obtained in 2mm sheets (Clarex®, Nitto Jushi Kogyo Co. Ltd, JP supplied by Weatherall Ltd, UK). Polylactic acid (PLA Ingeo™ Biopolymer 3100HP) was supplied in pellet form by Nature Works LLC (Minnetonka, MN).

Polylactic acid sheets preparation

To investigate the influence of the laser cut quality with respect to the physico-chemical characteristic of PLA, four sets of PLA sheets were prepared via compression moulding. Unlike PMMA which is available in sheets of different thicknesses, PLA is only available in films or pellets. To make PLA sheets, PLA pellets were dried for 6 hours at 80°C, and then collected in a sandwich composed by a metal frame (with dimensions: 11 cm width × 11 cm height, 2mm thickness) two TeflonTM films (50 μm in thickness, DuPontTM Teflon®) and two additional plates maintaining the assembly in place. Plates were pre-heated in manual hydraulic heated press (by Carver®, Inc.) to 210°C, that is slightly above the melting point of the pellets (200°C according to the supplier technical datasheet) and the sandwich with its frame was put between the heated plates. The stack containing the PLA pellet was maintained at 200°C, under pressure with the following cycle: 4 minutes under 10 bar, 30 seconds under 50 bar, 30 seconds under 100 bar and 30 seconds under 150 bar, so that a film with homogeneous thickness could be obtained. After this procedure, the heating system was switched off and the plates were cooled down to room temperature through cooling water, circulating in a serpentine located within the plates. Then, the pressure was released and the final sheet unpacked. Four sets were prepared by changing the cooling rate with the aim to achieve various crystallinities degree (the temperature time pressure protocol is available in suppl. info 1).

Sheets characterization by XRD

The prepared PLA sheets were analysed by X-ray Diffraction (XRD) using a PANalytcal® Empyrean with Cu kα radiation with a wavelength of λ= 154 nm, to determine quali-quantitative the crystallinity degree. A 2θ continuous scan type was used with a range from 5° to 80° to obtain the complete spectra of each sample.

Sheets characterization by DSC

The quantitative determination of the crystallinity degree was carried out using a DSC131 evo (Setaram Instrumentation, France). Each sample was heated from 30 °C to 250 °C with a heating rate of 10 °C/min, after a precondition at 30 °C for 10 minutes. As previously reported by (Naga et al.) [23] the crystallinity degree was estimated using the following equation (1):

$$X_c = \frac{(H_m - H_c)}{H_m^0} \times 100 \quad (1)$$

Where Hm and Hc are respectively the melting enthalpy and the crystallization enthalpy while H_m^0 is the theoretical melting enthalpy of a pure non-defective PLA crystal, 93 J/g.

Laser-cutting, Imaging and dimensional measurements

In order to investigate the laser cut-quality and to provide a practical guide when choosing laser cut manufacturing on PLA, a CO_2 commercial laser cutter (Epilog Mini Helix) with a 2 inch lens (101.6 μm beam spot) was used to produce slits through the PMMA and PLA sheets. Laser power, speed and frequency were chosen as input parameters to determine PLA laser cutting behaviours in terms of HAZ, kerf depth, width and kerf taper angle. To evaluate cut accuracy, recast layer, kerf depth and kerf width have been measured using a Dinolite microscope (Dino-Lite Premier2 AD7013MZT), while the determination of the heat affected zone was carried out using a polarized microscope (Olympus BX51). The determination of the kerf depth was carried out taking into account as input parameters laser power and speed, keeping the frequency, (number of pulses that the laser fires per second) constant to 5000 Hz, since their influence on the kerf depth carries more weight than the frequency. All the measurements were rounded to the first decimal to provide a practical guide in the selection of the parameters to use cutting a thickness specific sheet. Scanning Electron Micrography (SEM) was used to understand the topology of the laser-cut microchannels. To determine the laser cutting parameters, the width of the molten layer was measured on photographs acquired from a Dino-Lite Premier digital microscope. Kerf depth and kerf width were measured via image analysis with ImageJ from photographs taken by Dino-lite. HAZ was measured via polarised microscopy (Olympus). To evaluate surface roughness average (Ra), squares of 4 mm by 4 mm were engraved on the surface of ultra-high cooling rate (UHCR) and ultra-low cooling rate (ULCR) PLA and PMMA, and then analysed with a white light interferometer (ZYGO) with 1 nm resolution in vertical direction. The R_a quantitative determination was carried out using the software of the interferometer apparatus, Metro.Pro 8.2. To bind together the different PLA layers, a double sided adhesive tape (3M tape 469 MP) was used, unless further specified.

DNA binding to PLA and PMMA

To assess DNA binding to polylactic acid (PLA) and polymethyl-methacrylate (PMMA), Human Genomic DNA (Bioline) was diluted with water to 2ng/μl and 20ng/μl concentrations and incubated for 30 min with 8 mm^3 PLA and PMMA at room temperature. After incubation DNA concentration of samples and controls was measured with Qubit and Nanodrop in triplicates. Real time quantitative PCR was performed using 2x Power SYBR® Green PCR Master Mix (Thermo Fisher Scientific) to amplify 94 bp target with GAPDH primers (final concentration 200nM): forward 5'-AGGTTTACATGTTCCAATATGATTCCA-3' and reverse 5'-ATGGGATTTCCATTGATGACAAG-3'. The standard curve was created using a series of 5 serial dilutions of Human Genomic DNA, to assess the final concentration of the tested samples. Thermal cycling conditions involved a 10 minute cycle at 95°C followed by 40 cycles with 15 seconds at 95°C and 60 seconds at 60°C. Samples were amplified in duplicates using Mx3005P qPCR system (Agilent). Melting curve was performed as a control measure for non-specific amplification.

Chemicals leaching

To investigate the leaching of chemicals from both PLA and the benchmark material PMMA, molecular grade water was incubated at room temperature in the presence of 8 mm^3 cubes of PLA and PMMA for 30 minutes; and then the UV-VIS

spectrum was analysed using a microvolume spectrophotometer, Nanodrop instrument (ND-1000).

PCR inhibition

To evaluate PCR inhibition, three different concentrations (2 ng/µl, 10 ng/µl, 20 ng/µl) of genomic DNA samples were mixed together with 2x Power SYBR® Green PCR Master Mix, GAPDH primers (final concentration 200nM) and molecular grade water, and incubated with 8 mm^3 PLA and PMMA for 30 min on ice. A control without polymeric samples was prepared in the same way. The mixture was kept on ice to preserve the integrity of the polymerase contained in the PCR Master mix. After incubation qPCR was performed with the same conditions as described previously. Melting curve analysis was done to check the quality of amplified product. Linear regression analysis was done in MxPro qPCR software (R^2>0.98).

Electrode printing

The water-based biocompatible graphene ink was formulated from graphite via a previously published technique available in[24]. The final concentration of the graphene ink used for the inkjet printing was 2.70 mg/mL A Dimatix DMP-2800 inkjet printer (Fujifilm Dimatix, Inc., Santa Clara, USA) was used to print electrodes on both PLA and PMMA substrates. Prior to printing, the substrates were cleaned with ethanol followed by drying under N_2 flow. The nozzle plate consists of a single raw of 16 nozzles with a 23 µm diameter, spaced 254 µm apart, with typical drop size of 10 pL. The electrodes were printed onto the substrates at 40 °C with 35 mm spacing between the drops. The number of printing passes for all the electrodes was 60.

Electrode testing

The graphene electrodes printed on PLA and PMMA substrates and embedded in 1 mm wide and 0.8 mm high PLA microfluidic channels were electrochemically characterised with an Autolab PGSTAT 128N potentiostat (Metrohm Autolab, Herisau, Switzerland) controlled with Nova 2.1.2 software by recording cyclic voltammograms (CV) in the presence of 5 mM potassium ferricyanide and 5 mM potassium ferrocyanide in 0.1 M KCl solution and 0.1 M KCl solution as well as without potassium ferricyanide and potassium ferrocyanide (negative control) at 10 mV/s scan rate.

Statistical analysis

All statistical tests were performed with the student's t-test unless otherwise stated

RESULTS AND DISCUSSION

PLA laser cutting quality

CO_2 laser cutting is an established material manufacturing technology, widely used due to its low cost and rapidity, and good quality depending on the material. This technique has been applied to both metallic and non-metallic materials e.g. glass, woods, thermoplastics, thermosets and elastomers.[25,26,27] During cutting, the laser beam is focused onto the material surface, causing a localised melting and/or vaporization.[28] The heat generated by the laser diffuses through the material altering its microstructure and properties in an area named Heat Affected Zone (HAZ) (Figure 2 A-i). The HAZ is strictly related to the thermal properties of the material (e.g. thermal diffusivity), its thickness and the laser power, speed and frequency. In addition, the presence of a recast layer (or burr), close to the cut, depends on the beam energy, gas pressure and exact laser cutting mechanism taking place.[29] Different methodologies have been developed to evaluate how a polymeric material's behaviour interacts with laser machining. The HAZ dimensions, recast layer, surface roughness, dimensional precision, kerf quality and mechanical properties after laser cutting can help to determine whether a material has good workability or not. The laser workability differences between different polymers arise from differences in their molecular structures, thermal properties (latent heat of vaporisation, melting enthalpy, specific heat), laser beam absorptivity and degree of crystallinity. In general, the cutting of thermoplastics is principally achieved by fusion cutting, except in the case of PMMA where the main process involved is vaporization.[30] PMMA is commonly used, in conjunction with laser-based rapid-prototyping techniques, due to its optical transparency and good CO_2 laser workability.[31,32]In contrast, it has been shown that CO_2 laser cutting of PLA occurs through a combination of melt shearing and vaporization.[33,34] We compared the workability of 2mm thick PMMA ((Figure 2 A-ii and A-iii) and PLA sheets (Figures 2 A-iv and A-v) and found that PLA has a reduced workability, as exemplified by the large recast layer in the PLA cut (about 90 µm high) on as opposed to PMMA cut for the same laser parameters (frequency, power, speed) which has no recast layer. Furthermore, we observed thermal deformation of PLA due to the high energy of the laser and the lower thermal diffusivity under lower speed. This constrains the operator to using high speed at the cost of a higher number of passes to obtain a cut-through feature (data not shown).

Investigating the laser workability of PLA with different crystallinity degree

The large recast layer produced in the laser-cut PLA sample makes this material impractical for use in the context of a layer-by-layer prototyping technique due to a reduced surface contact during the assembly. However, we hypothesised that the PLA polymer structure could be manipulated to reduce the HAZ and, in particular the recast layer, so as to produce better cut quality, compatible with a layer-by-layer assembly developed in (Liga 2016).

To investigate this hypothesis, four types of PLA sheets were produced with differing degrees of crystallinity using a compression moulding technique: Ultra High Cooling Rate (UHCR), High Cooling Rate (HCR), Low Cooling Rate (LCR) and Ultra Low Cooling Rate (ULCR) (Suppl. info1). The purpose was to investigate the influence of the cooling protocol on the overall morphology on the nanoscale (size of crystal lamellae) and on the mesoscale (size and amount of crystalline aggregates such as spherulites), (according to Continuous Cooling Transformation proposed for polymeric materials[35]) and, in turn, to study the behaviour of these different PLA types when subjected to CO_2 laser-cutting. During the phase transition from liquid to solid, a rapid cooling rate does not provide the time necessary for crystallites to form and, by freezing the polymer into a disordered structure, generates an amorphous status. As expected, we were able to tune the nanoscopic architecture and the molecular structure and obtain four materials with varying degrees of crystallinity as evidenced by XRD and DSC analysis (Suppl.info 1). Fast cooling rates (UHCR and HCR protocols) led to the formation of amorphous

A – Workability of PMMA versus native PLA

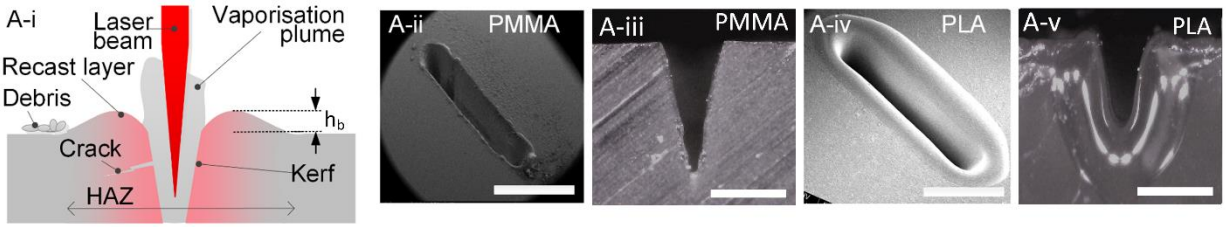

B – Workability of PLA with varied crystallinity degrees

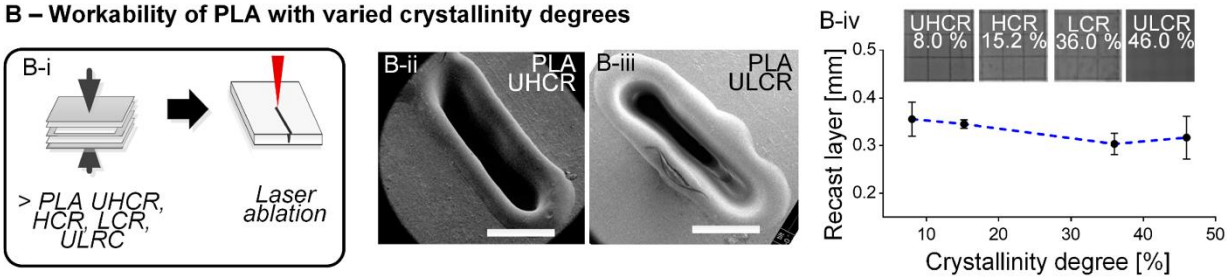

C- Workability of PLA with different laser parameters

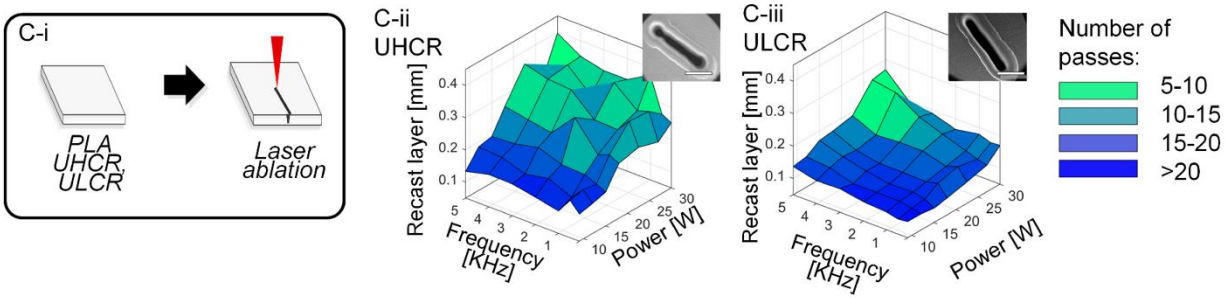

D- Workability of PLA at sub-zero temperatures

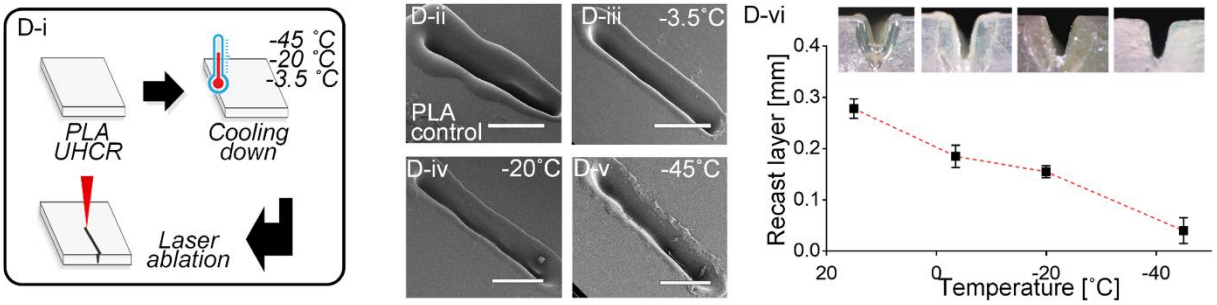

E- Workability of protected PLA (Sacrificial Layer Assisted Manufacturing: SLAM)

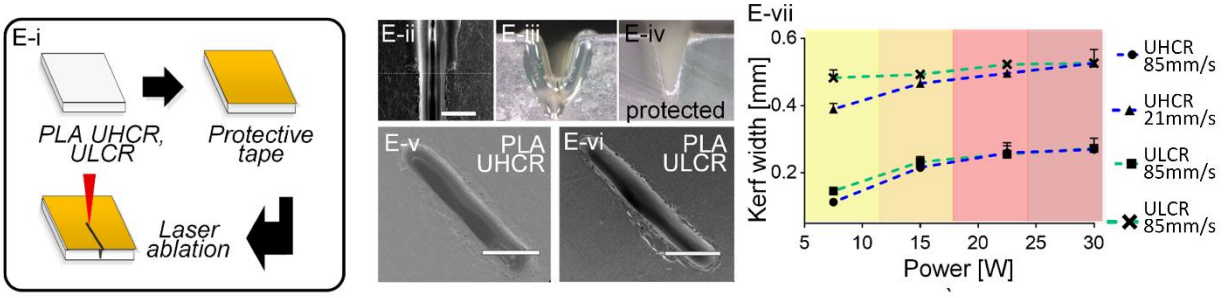

Figure 2: Laser workability of PLA. (A) Workability of PMMA versus native PLA, (A-i) Laser cutting process. w_k reperesents the kerf width, h_b the burr height (A-ii) SEM picture of laser ablated PMMA (S: 85mm/s; P:15 W; F:5000 Hz), scale bar is 1mm (A-iii) Cross section of the PMMA kerf, scale bar 0.6 mm (A-iv) SEM picture of laser ablated PLA (S: 85mm/s; P:15 W; F:5000 Hz) scale bar is 1mm (A-v) Cross section of the PLA kerf, scale bar 0.6 mm. (B-i) Workability of PLA with varied crystallinity degree, (B-ii) SEM picture of laser ablated UHCR PLA (S: 85mm/s; P:15 W; F:5000 Hz), scale bar is 0.8 mm, (B-iii) SEM picture of laser ablated ULCR PLA (S: 85mm/s; P:15 W; F:5000 Hz), scale bar is 0.8 mm, (B-iv) Recast layer width in function of the crystallinity degree of the produced PLA sheets, in insert pictures of the prepared sheets. (C-i) Workability of PLA with different laser parameters, (C-ii) Recast layer width of UHCR sheet in function of the laser power and frequency, in insert SEM picture of the UHCR sheet (S: 85mm/s; P:15 W; F:2500 Hz), (C-iii) Recast layer width of ULCR sheet in function of the laser power and frequency, in insert SEM picture of the ULCR sheet (S: 85mm/s; P:15 W; F:2500 Hz); (D-i) Workability of PLA at sub-zero temperature, (D-ii) SEM picture of laser ablated UHCR at room temperature (S: 21.25 mm/s; P: 22.5 W; F:5000 Hz), scale bar 0.8 mm, (D-iii) SEM picture of laser ablated UHCR at -3.5 ˚C (S: 21.25 mm/s; P: 22.5 W; F:5000 Hz), scale bar 0.8 mm, (D-iv) SEM picture of laser ablated UHCR at -20 ˚C (S: 21.25 mm/s; P: 22.5 W; F:5000 Hz), scale bar 0.8 mm , (D-v) SEM picture of laser ablated UHCR at -45 ˚C (S: 21.25 mm/s; P: 22.5 W; F:5000 Hz), scale bar 0.8 mm, (D-vi) Recast layer width of UHCR sheet in function of the starting working temperature, in insert cross section picture of the samples cut with different starting temperature; (E) Workability of protected PLA, (E-ii) SEM picture of the laser kerf on protected and unprotected UHCR (S: 21.25 mm/s P: 22.5 W F: 5000 Hz), scale bar is 0.5 mm; (E-iii) cross section picture of the unprotected UHCR cut, (E-iv) cross section picture of the protected cut, (E-v) SEM picture of laser ablated protected UHCR (S: 21.5 mm/s P: 22.5 W F: 5000 Hz), scale bar is 1 mm, (E-vi) SEM picture of laser ablated protected ULCR (S: 21.25 mm/s P: 22.5 W F: 5000 Hz), scale bar is 1 mm, (E-vii) Kerf width in function of the laser power of UHCR and ULCR at fixed frequency (F: 5000 Hz), and two different speed (S: 85 mm/s and 21.25 mm/s). The kerf depth, kd, associated is (from left to right) kd: 1.6-0.5 mm (first zone), kd: 0.9-0.3 mm (second zone); 0.6-0.15 mm (third zone), 0.4-0.1 mm (forth zone).

sheets while lower cooling rates (LCR and ULCR protocols) resulted in semi-crystalline sheets. The degrees of crystallinity for the PLA sheets produced using the UHCR, HCR, LCR and ULCR protocols, were determined to be around 8, 15, 36 and 46 % respectively. However, we found that the crystallinity degree of PLA did not influence the recast layer on 2 mm cuts made in material obtained with the UHCR, HCR, LCR, and ULCR protocols at the same frequency, speed and power, respectively 5000 Hz, 85 mm/s and 15 W (Figure 2B). The UHCR protocol gave the best transparency (insets in Figure 2 B-iv) and was preferentially use for the rest of the study, alongside the ULCR protocol for comparison.

Influence of laser power on PLA workability

Since the crystallinity did not influence the recast layer height, we investigated if the laser power would have the effect desired (reduced recast layer) while the laser head speed was kept at the maximum value (85 mm/s). Although it was possible to reduce the width of the recast layer to 95 µm in cut-through samples, up to 25 several beam passages were required (Fig. 2 C-ii,iii), hence reducing the practicality of the technique and its rapid-prototyping credentials.

Investigating the laser workability of PLA at different temperature

As a different solution, we hypothesised that cooling the material prior to the cutting process, could reduce the flow of melted material, and therefore prevent or reduce the undesired recast layer (fig. 2 D-i). We cooled 2 mm PLA sheets, for 30 min at -3.5°C, -20°C and -45°C respectively, on ice, in a freezer and on dry ice, prior to cutting 2 mm long slits at set parameters (S: 21.25 mm/s, P: 22.5 W). Cooling the material from room temperature to – 45˚C resulted in an 85% decrease in the size of the recast layer in conjunction with a decrease in the kerf width (Figure 2B, suppl. Information 2). Due to significant decrease in recast layer, a lower cutting speed (21.25 mm/s, enabling just two passes for cut-through) was used in this experiment. However, although this method proved successful (fig 2 D-iii,iv,v,vi), material deformations were still observed. Furthermore, the additional step involving storage of the material at -45˚C prior to prototyping, limits the usefulness of this technique.

Investigating the laser workability of PLA with a protective tape: Sacrificial Layer Assisted Manufacturing (SLAM)

A third solution was investigated and involved the application of adhesive tape as a sacrificial layer (Figure 2 E-i) which was placed on the material prior to laser cutting.[36,37] It was hypothesised that the film would provide a thermal shield, spreading the heat out onto the whole surface thereby effectively decreasing the laser beam absorptivity of the system. A 100 µm thin paper tape was applied across the material and resulted in the complete absence of a recast layer (Figure 2 D-ii), regardless of the choosen laser power, speed and frequency. Pits, of approximately 20 µm diameter, were observed on the external edges of the slits (suppl. Info 3). We were not able to measure how deep were these pits, however they are reminiscent of nanopits reported in another publication[38]. The absence of recast layer was observed on PLA of various crystallinity degrees (Figure 2 E-ii and E-iv,v,vi). Various tapes and thicknesses were tested. The thickness of the tape influences the final shape of the kerf (suppl. Info 3). Paper tape used for masking was found to be safer and easier to remove from PLA once cut, than plastic tapes. This SLAM method, using a protective paper tape adhesive of 100 µm thickness, was used in the rest of this study.

Influence of laser cutting power and speed on kerf width and taper angle with SLAM

Measurements of kerf depth and width for cuts produced in protected, 2 mm, PLA sheets (UHCR and ULCR) when using a range of laser speeds (21.25 – 85 mm/s) and powers (7.5-30 W) reveal that the laser cut features are not influenced by the degree of crystallinity of the PLA sheets (Figure 2 E-vii and Suppl. info 4). At higher powers, deeper and larger cuts were observed. Similar effects were obtained by operating at lower speeds. The influence of speed on kerf depth is greater than that of power until the cutting velocity falls below 42.5 mm/s. This is probably due to power dispersion in the system.

A model to describe the effect of the tape and predict the kerf profile

In order to predict the kerf profile in function of ablation parameters (speed and power) a semi-empirical model has been developed, derived from a mathematical model previously reported by Kumar et al.[39,40] In their work, the prediction of kerf profile and depth in PMMA material was based on an energy balance which assumed that the energy provided by the laser was absorbed by the material and sufficient to raise the surface temperature and vaporise it. The only thermal process considered in this model was vaporisation, while PLA is cut via a combination of vaporisation and melt shearing. In the new model for PLA ablation, we modified the energy balance to consider that the heat provided to the material lead to melting and vaporisation phenomena. The full developed model for the kerf profile is available in Suppl.Info 5. The comparison between the kerf shape model prediction and the experimental results for four different laser speeds on UHCR PLA with and without the application of the sacrificial layer is shown in suppl info 5. The percentage error in the prediction of the maximum kerf depth for the developed model is 5 %. This model will allow future users to accurately predict cut profiles in PLA materials

Suitability of PLA for biological protocols

The difference in surface roughness is a key feature of a laser-cut PLA microchannel versus a PMMA channel. We investigated the influence of the ULCR and HCR manufacturing protocols on the surface roughness and compared this to a PMMA standard sample. CO_2 laser cutting of PMMA leads to the formation of porous structures in the working zone due to the vaporisation process taking place. In contrast, during the laser cutting of PLA the melting process prevails over the vaporisation one.[41,42] The outcome is that a smoother channel surface is achieved for PLA with respect to PMMA (Figure 3A, B). An interferometry analysis (Figure 3C) has shown that, when using the same protocol, the average Ra of PMMA is of the order of 3 µm while for PLA is 0.3 µm (Fig 3). This order of magnitude difference in surface roughness between PMMA and PLA will undoubtedly create new opportunities in the use of PLA for the rapid prototyping and production of microfluidic devices, showing comparable features with mass manufacturing techniques. Firstly, reduced wall roughness, may enable better flow properties such as a higher critical Reynolds number for transition from laminar to turbulent flow and no local recirculation.[43] Secondly, the smoother channel surface will considerably decrease molecular adsorption as surface to volume ratios will be minimised. The non-specific adsorption of molecules is a recurring concern for microfluidic designers and diverse solutions have been

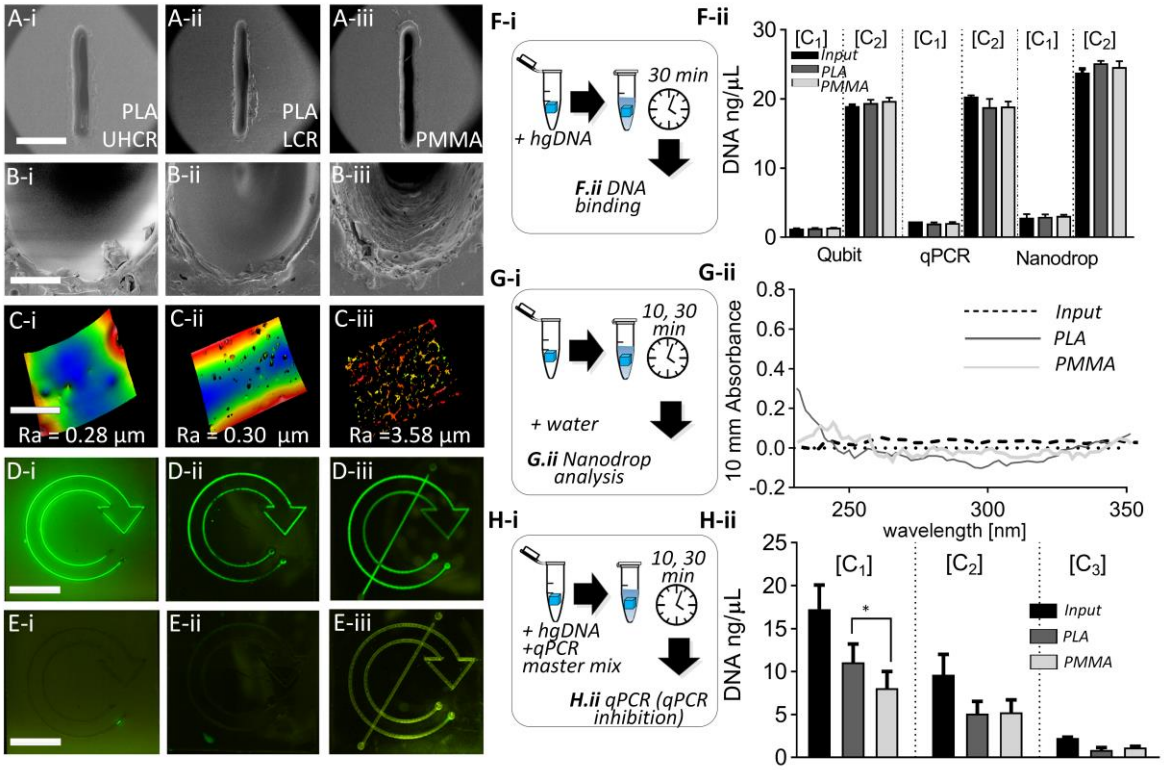

Figure 3: (A) SEM picture of top view of a slit cut with power 15 W, speed 42.5mm/s and frequency 5000 Hz on (A-i) protected UHCR PLA, (A-ii) protected ULCR PLA and (A-iii) PMMA. Scale bar is 1 mm. As can be seen no substantial different are present between the PLA samples and PMMA one. (B) SEM images of top view of channel ends. (B-i) UHCR PLA, (B-ii) ULCR PLA, (B-iii) PMMA. Scale bars are 100 µm. Pore formation can be noticed in PMMA cut edge. (C) Surface roughness from Interferometer analysis UHCR PLA (C-i), ULCR PLA (C-ii) and and PMMA (C-iii). Scale bar is 0.50 µm. (D) Photographs acquired with a Dinolite fluorescent microscopes microscopes on ULCR PLA (D-i), UHCR PLA (D-ii) and on PMMA (D-iii) after injecting fluorescein inside the channel and washing the channel with DI water (E-i,iii). (F-i) Protocol for DNA binding. (F-ii) Non-specific DNA binding Qubit results, qPCR and nanodrop results. (G-i) Protocol for leaching experiment. (G-ii) Leaching experiments results. (H-i) Protocol for qPCR inhibition. (H-ii) qPCR inhibition results.

deployed in an attempt to overcome this problem.[44] Non-specific adsorption can lead invariably to a loss of molecular markers or reduced assay performance. For example, the PCR inhibition noted when using some polymeric systems (e.g. Silicon, PDMS and PMMA) has been attributed to polymerase adsorption on the channel walls.[45] In order to compare the non-specific molecular binding properties of PLA and PMMA laser cut channels, the microchannels in two equivalent microfluidic devices were filled with a solution of fluorescein (5 mg/mL), incubated for 30 min and imaged (Figures 3 D-i, D-ii and 3 D-iii). Subsequently, the channels were flushed with 10 mL of de-ionised (DI) and re-imaged (Figures 3 E-i, E-ii and 3 E-iii). Analysis of the fluorescent images showed that after washing the PMMA channels had retained on average 18% of the initial fluorescein while the PLA channels had retained only 5%. This finding supports our expectation that the smoother channel surfaces obtained with PLA result in decreased molecular adsorption relative to PMMA and, therefore, demonstrates an additional advantage of sustainable PLA devices over PMMA systems.

Non-specific DNA binding to bulk PLA material was also investigated and compared to PMMA. Cubes of 8 mm^3 of each material (PLA and PMMA) were incubated for 30 minutes in aqueous solutions containing two different concentrations of Human Genomic DNA (2ng/µL and 20ng/µL) (Figure 3 F-i). The tested samples and the control concentrations of hgDNA were measured by Qubit fluorescence measurement, Real-time quantitative PCR (qPCR) and with Nanodrop spectrophotometer as per method section. No significant unspecific binding was detected at either concentration in the presence of PMMA and PLA using both measurement methods (Figure 3 F-ii).

Leaching of polymeric components from the bulk material is another issue in microfluidic systems. Although the mobility of low molecular weight oligomers in the whole polymer is known, few studies have looked into this potential problem in detail [28]. It has been suggested that this uncontrolled and undesired leaching could lead to cytotoxicity, interference with cellular signaling pathways or PCR inhibition.[46] To investigate differences in leaching between the benchmark material PMMA and PLA, molecular grade water was incubated at room temperature in the presence of 8 mm^3 cubes of PLA and PMMA for 30 minutes. The 260 and 280 nm wavelengths absorbance of the water from each sample were then analysed using a microvolume spectrophotometer, Nanodrop instrument, to assess the presence of leached molecules that could negatively interact in the quantification of nucleic acids[19],[46] (Figure 3 G-i and G-ii). The absorbance spectrum indicates that both PLA and PMMA are almost inert. (Figure 3 G-ii). Finally, it has been suggested that qPCR inhibition by polymers might be induced by polymerase inhibition rather than non-specific binding.[45,47] Here qPCR inhibition was evaluated by incubating the polymerase in presence of PMMA or PLA materials. Solutions containing template hgDNA at three different concentrations, PCR master mix and a 8 mm^3 cube of PMMA or PLA, were incubated for 30 minutes at room temperature. PLA and PMMA materials were found to produce comparable inhibition at hgDNA concentrations of 2 ng/µl and 10 ng/µl (Figure 3 H-i and H-ii). At higher concentrations of hgDNA (20 ng/ µL), PCR

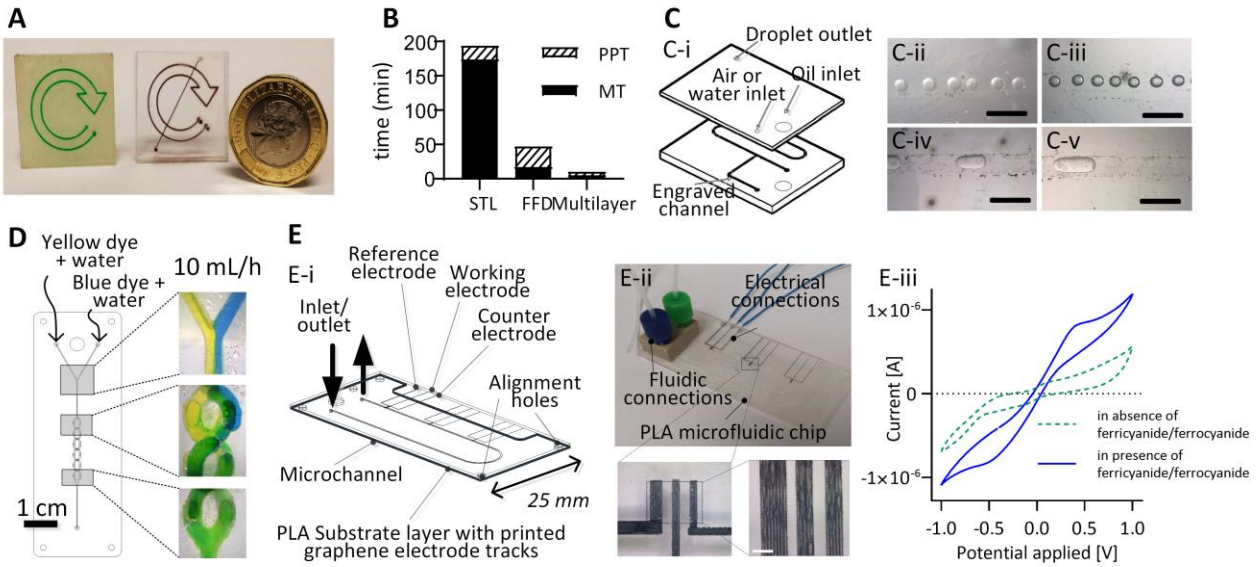

Figure 4: (A) 3 layers microfluidic "recycle" sign. Left ULCR PLA, right PMMA (B) Manufacturing time comparison between three different rapid prototyping techniques for the production of the microfluidic "recycle" sign. STL(stereolithography), FFD (fusion filament deposition) and Multi-layer (involving the CO_2 laser cutting of PLA sheets in a micro-structured layer that are bonded together with a double-sided adhesive tape). (C) Two-layer microfluidic device for the production of water-in-oil and air-in-oil droplets. (C-i) Blow-up view of the chip design. (C-ii) Water in oil droplet, flow rate ratio 0.1; (C-iii) Air in oil droplet, flow rate ratio 0.1; (C-iv) Water in oil droplet, flow rate ratio 1; air in oil droplet, flow rate ratio 1. Scale bar is 1mm. (D) Five layers Micromixer device. (E) Three layer hybrid microfluidic device; E-i) schematic representation of the device; E-ii) on the top photograph of the final prototype device, on the bottom left picture of the printed electrodes on PLA, on the right particular of the water inject printed graphene electrodes. Scale bar is 0.2 mm. E-iii) Electrochemical characterization of the hybrid device with a Cyclic Voltammetry (CV) at 10 mV/s scan rate. Blue straight line CV in presence of Ferricyanide/Ferrocyanide, green dot line in absence of Ferricyanide/Ferrocyanide.

inhibition was higher ($p<0.05$) when the polymerase was incubated with PMMA than PLA.

In conclusion, PLA has been found to be comparable or better than the commonly employed, non-sustainable material of PMMA in terms of roughness following laser-cutting, leaching, non-specific binding and PCR inhibition.

PLA-based multi-layer microfluidic cartridges

The ability to precisely laser-cut PLA sheets can be applied to the fabrication of multi-layer disposable components, of varying complexities and functionalities, such as microfluidic chips. Examples of such components have been prepared using PLA and PMMA and feature 2 and 3 layers, respectively, as shown in Figure 4A. Each layer was cut from 2 mm sheets and manually assembled (see Method section for details). The PLA device represents the first attempt to fabricate a multi-layer device from this material using a laser-cut, laminated technique. The prototyping times for fabrication of the same design using three different techniques have been compared. The techniques investigated were our established multi-layer technique and two additive manufacturing solutions, fused deposition modelling and stereolithography. The time to post-process each part was included as it is a recognised challenge in the production of 3D printed microfluidic devices.[17,48] We found that our technique was at least 2 times faster than other 3D printing techniques, (Figure 4B). Due to the transparency of the UHCR PLA sheet (Suppl Info 1), imaging of our prototypes, as required for several biomedical applications, is possible. On the contrary, when PLA is 3D printed via FFD a multi-material solutions (e.g. glass observation window) had to be devised for imaging in microfluidic circuits.[16,49] Droplet production is another common microfluidic functionality. On-site microdroplet production in disposable, single-use devices are highly desirable, for example for enhanced ultrasound imaging at the point of administration. Droplet production has been successfully integrated into PLA-derived microfluidic systems and tested at a range of flow rate ratios (Figure 4C). Mixing is also needed in most biochip protocols. This was achieved in the PLA device using a five-layer split & recombine mixer at 10mL/hr (Figure 4D).

Finally, to broaden the demonstration of possible functionalities on single-use point of care devices, low environmental impact water-based graphene inks[24] were used to produce electrodes directly on the surface of PLA samples and integrated into a device in the view to enable analytical functionalities such as sensing (Figure 4 E-i and E-ii). These electrodes were integrated into a microfluidic channel. Cyclic Voltammetry allows monitoring of redox behaviour of chemical species. In particular, ferricyanide/ferrocyanide redox reaction is commonly used in electrochemistry to assess electrode functionality.[50] A solution containing 5 mM Potassium ferricyanide and Potassium ferrocyanide was introduced inside the channel and redox currents were measured as per Method section. The resulting voltammogram (blue, Figure 4 E-iii) showed a clear Potassium ferricyanide reduction and Potassium ferrocyanide oxidation peak, while a negative control in the absence of Potassium ferricyanide/ferrocyanide (green, Figure 4 E-iii) showed no peaks, thereby confirming of the graphene electrodes on the PLA substrate function as expected and that no further modifications are necessary.

OUTLOOK

We have developed a method enabling a complete, sustainable, and low-carbon footprint lifecycle, for single-use, disposable, medical microcomponents. Starting from a polymer material derived from renewable sources, PLA, sheets of material of various thicknesses and physicochemical properties were produced. The CO_2 laser workability was improved by using a sacrificial layer method (SLAM) to completely eradicate the recast layer normally present on the cut material. The laser-cut sheets were then assembled into multi-layered components using double-sided adhesive tape. Using this rapid prototyping technique, complex devices were rapidly produced and tested. We have demonstrated the use of these multi-layer components to form complex 5 layer microfluidic mixers and devices for microdroplet production. When the development of the device is completed, providing a good design for manufacture approach has been followed, a device could be mass-manufactured in the same material, PLA, with very limited design changes, using microinjection moulding or other suitable techniques. PLA-based single-use medical microscale components have a low carbon footprint and additive-free PLA can be incinerated safely in rudimentary setting. We envisage that other techniques with sustainability credentials, such as paper microfluidics could be used in a non-competitive way with polymeric material as each will have their own niche applications. The two materials might also be used together to benefit from a wider range of functionalities. Ultimately, the sustainability, and in particular the ability to incinerate any material in a safe way will depend on the addition of additives to the raw material. In that regard, the control of biopolymer production and quality controls by regulators will be important in producing PLA material for truly sustainable and safe material for medical applications.

ASSOCIATED CONTENT

The supplementary informations material is available free of charge via the Internet at http://pubs.acs.org."
DSC and XRD analysis of the prepared PLA sheets; laser workability of PLA at different temperatures; Investigation of the laser workability with protective tape of different thickness; Influence of the crystallinity degree on the kerf depth and width on ablated protected PLA; A mathematical model to predict kerf profile; FTIR spectra of PLA and of the paper tape

AUTHOR INFORMATION

Corresponding Author

* m.kersaudy-kerhoas@hw.ac.uk

Author Contributions

AO performed all experiments but the electrode printing, electrochemical measurements and biological measurements, and contributed to the analysis of the results
IK performed all biological experiments and contributed to the analysis of the results
AL contributed to the analysis of the results,
GC contributed to the material characterisations
SC contributed to the literature on lifecycle analysis of PLA
HS performed the electrochemical measurement
TB contributed to the reagents and materials and the analysis of the electrochemical measurement results

KP printed the electrodes
CC contributed to the reagents and materials and the conception and analysis of the electrodes printing results
NH, VLC and MKK conceived and designed the study and contributed to the analysis of the results
The manuscript was written by AO, NH and MKK in close consultation with all authors. The manuscript was written through contributions of all authors. / All authors have given approval to the final version of the manuscript.

ACKNOWLEDGMENT

A.O and A.L are funded by a James Watt scholarship. I.K. is funded by a Medical Research Scotland studentship. MKK receives funding from the Royal Academy of Engineering, the Royal Society and the Engineering and Physical Sciences Research Council EP/R00398X/1. CC and KP acknowledge the Grand Challenge EPSRC grant EP/N010345/1. We would like to thank Mark Leonard for assistance with the SEM imaging and Prof Valeria Arrighi and Filipe Vilela for access to equipment.

REFERENCES

1. Point-of-Care Diagnostics Market by Products (Glucose, Cardiometabolic Monitoring, & Infectious Disease Testing Kits, Cardiac & Tumor Markers), End Users (Home, Hospitals, Ambulatory Care), Over-the- Counter & Prescription Based - Global Forecast to 2021. https://www.marketsandmarkets.com/Market-Reports/point-of-care-diagnostic-market-106829185.html. Report Code: MD 2702 (accessed July, 2016).

2. Singh, P. & Sharma, V. P. Integrated Plastic Waste Management: Environmental and Improved Health Approaches. *Procedia Environ. Sci. 2016,* **35,** 692–700. doi:10.1016/j.proenv.2016.07.068

3. Unger,S. R., Hottle,T. A., Hobbs,S. *R., Thiel,C. L., Campion,N., Bilec,M. M., Landis,A. E.* Do single-use medical devices containing biopolymers reduce the environmental impacts of surgical procedures compared with their plastic equivalents ? *Journal pf Healtth Services and Policy. 2017,* **0,** 1–8. doi: 10.1177/1355819617705683

4. Sullivan, J.B., Krieger, G.R. Clinical Environmental Health and Toxic Exposures, 2nd Edition,Lippincott Williams & Wilkins: Philadelphia, (2001).

5. Awodele, O., Adewoye, A. A. & Oparah, A. C. Assessment of medical waste management in seven hospitals in Lagos , Nigeria. *BMC Public Health. 2016,* 1–11. doi:10.1186/s12889-016-2916-1

6. Yang, C., Peijun,L., Lupi,C., Yangshao,S., Diandou, X., Qian,F., Shasha,F., Sustainable management measures for healthcare waste in China. *Waste Management*.2009,**29,**1996–2004. doi:10.1016/j.wasman.2008.11.031

7. Da Silva, C. E., Hoppe, A. E., Ravanello, M. M. & Mello, N. Medical wastes management in the south of Brazil. *Waste Management*. 20045, **25,** 600–605. doi:10.1016/j.wasman.2004.03.002

8. Castro-aguirre, E., Iñiguez-franco, F., Samsudin, H., Fang, X. & Auras, R. Poly (lactic acid) — Mass production , processing , industrial applications , and end of life ☆. *Adv. Drug Deliv. Rev.* 2016. doi:10.1016/j.addr.2016.03.010

9. Vink, E. T. H., Rábago, K. R., Glassner, D. A. & Gruber, P. R. Applications of life cycle assessment to NatureWorks™ polylactide (PLA) production. *Polym. Degrad. Stab. 2003,* **80,** 403–419. doi:10.1016/S0141-3910(02)00372-5

10. Vink, E. T. H., Glassner, D. a., Kolstad, J. J., Wooley, R. J. & O'Connor, R. P. ORIGINAL RESEARCH: The eco-profiles for current and near-future NatureWorks® polylactide (PLA) production. *Ind. Biotechnol.2007,* **3,** 58–81.

11. North, E. J. & Halden, R. U. Plastics and environmental health: The road ahead. *Rev. Environ. Health. 2013,* **28,** 1–8. doi:10.151/reveh-2012-0030

12. Chien, Y.-C., Liang, C., Liu, S.-H. & Yang, S.-H. Combustion kinetics and emission characteristics of polycyclic aromatic hydrocarbons from polylactic acid combustion. *J. Air Waste Manag. Assoc.2010,* **60,** 849–855. doi:10.3155/1047-3289.60.7.849

13. Rayna, T. & Striukova, L., From rapid prototyping to home fabrication : How 3D printing is changing business model innovation. *Technol. Forecast. Soc. Chang.2016,***102,**214–224. doi:10.1016/l.techfore.2015.07.023

14. Jiang, R., Kleer, R. & Piller, F. T., A Delphi study on economic and societal implications of 3D printing for 2030. *Technol. Forecast. Soc. Chang.* 2017, **117,** 84–97.doi:10.1016/l.techfore.2017.01.006

15. Malinauskas M., Rekštytė S., Lukoševičius L., et al. 3D Microporous Scaffold Manufactured via Combination of Fused Filament Fabrication and Direct Laser Writing Ablation. *Micromachines*. 2014, **5,** 839-858. doi:10.3390/mi5040839.

16. Morgan, A.J.L., San Jose, L.H., Jamieson, W.D., *et al.* Simple and versatile 3D printed microfluidics using fused filament fabrication. *PLoS One* . 2016, **11,** 1–17. doi:10.1371/journal.pone.0152023

17. Waheed,S., Cabot, J.M., Macdonald, N.P., *et al.* 3D printed microfluidic devices: enablers and barriers.

Lab Chip, 2016, **16,**1993–2013. doi:10.1039/C6LC00284F.

18. Macdonald,N.P., Cabot,J.M., Smejkal,P., Guijt, R.M., Paull, B., Breadmore, M.C., *et al.* Comparing Micro fluidic Performance of Three-Dimensional (3D) Printing Platforms. *Anal Chem*. 2017;**89,**3858-3866. (2017). doi:10.1021/acs.analchem.7b00136

19. Walsh, D. I., Kong, D. S., Murthy, S. K. & Carr, P. A. Enabling Microfluidics: from Clean Rooms to Makerspaces. *Trends Biotechnol.2017,* **35,** 383–392. doi:10.1016/j.tibtech.2017.01.001

20. L. Fu, W. Ju, R. Yang, Y. Wang, Rapid prototyping of glass-based microfluidic chip utilizing two-pass defocused CO2 laser beam method, *Microfluid Nanofluid*. 2013, **14,** 479-487. doi:10.1007/s10404-012-1066-8.

21. Liga, A., Morton, J. A. S. & Kersaudy-Kerhoas, M. Safe and cost-effective rapid-prototyping of multilayer PMMA microfluidic devices. *Microfluid. Nanofluidics. 2016,* **20**. doi:10.1007/s10404-016-1823-1

22. Arnette, A. N., Brewer, B. L. & Choal, T. Design for sustainability (DFS): the intersection of supply chain and environment. *J. Clean. Prod.* 2014, **83,** 374–390.doi:10.1016/j.jclepro.2014.07.021

23. Naga, N., Yoshida, Y., Noguchi, K. & Murase, S. Crystallization of Amorphous Poly(Lactic Acid) Induced by Vapor of Acetone to Form High Crystallinity and Transparency Specimen. *Open J. Polym. Chem. 2013,* **3,** 29–33. doi:10.4236/ojpchem.2013.32006

24. Mcmanus, D., Vranic, S., Withers, F., *et al.* Water-based and biocompatible 2D crystal inks for all-inkjet-printed heterostructures. *Nat. Nanotechnol.* 2017, **12,** 343–350. doi:10.1038/nnano.2016.281.

25. Zhou, B. H. & Mahdavian, S. M. Experimental and theoretical analyses of cutting nonmetallic materials by low power CO2-laser. *J. Mater. Process. Technol. 2004,* **146,** 188–192. doi:10.1016/j.matprotec.2003.10.017

26. Davim, J. P., Barricas, N., Conceição, M. & Oliveira, C. Some experimental studies on CO2 laser cutting quality of polymeric materials. *J. Mater. Process. Technol. 2008,* **198,** 99–104. doi:10.16/j.jmatprotec.2007.06.056

27. Isiksacan, Z., Guler, M. T., Aydogdu, B., Bilican, I. & Elbuken, C. Rapid fabrication of microfluidic PDMS devices from reusable PDMS molds using laser ablation. *J. Micromech. Microeng. 2016,* **26.** doi:10.1088/0960-1317/26/3/035008

28. Vasiga, D. A Review of Carbon Dioxide Laser on Polymers. *Internationl Journal of Engineering and Technology. 2015,* **4,** 874–877.

29. Davim, J. P. Laser Beam Machining, *Nontraditional machining processes: Research advances*. *Nontraditional Machining Processes: Research Advances*. 2013 doi:10.1007/978-1-4471-5179-1

30. Caiazzo, F., Curcio, F., Daurelio, G. & Minutolo, F. M. C. Laser cutting of different polymeric plastics (PE, PP and PC) by a CO 2 laser beam. *J. Mater. Process. Technol. 2005,* **159,** 279–285. doi:10.1016/j.jmatprotec,2004.02.019

31. Klank, H., Kutter, J. P. & Geschke, O. CO(2)-laser micromachining and back-end processing for rapid production of PMMA-based microfluidic systems. *Lab Chip, 2002,* **2,** 242–246. doi:10.1039/b206409j

32. Hong T-F, Ju W-J, Wu M-C, Tai C-H, Tsai C-H, Fu L-M. Rapid prototyping of PMMA microfluidic chips utilizing a CO2 laser. *Microfluid Nanofluidics*.2010, **9,** 1125-1133. doi:10.1007/s10404-010-0633-0.

33. Anto, A. J., St, B. & Szustakiewicz, K., et al. Effect of CO 2 laser micromachining on physicochemical properties of poly (L -lactide). *Second International Conference on Applications of Optics and Photonics, 2014,* **9286,** 1–10. doi:10.1117/12.2063684

34. Malinauskas, M., Lukosevicius, L.,Butkus, S. & Paipulas, D. Femtosecond Pulse Light Filament-Assisted Microfabrication of Biodegradable Polylactic Acid (PLA) Material.*Journal of laser Micro/Nanoengineering,*2015,**10,**222-228 doi:10.2961/jlmn.2015.02.0021

35. Brucato, V., Kiflie, Z., Carrubba, V. L. A., Piccarolo, S. & Chimica, I. The Continuous Cooling Transformation (CCT) as a Flexible Tool to Investigate Polymer Crystallization under Processing Conditions. 2009, **28,** 86–119.doi:10.1002/adv

36. Stępak, B., Antończak, A.J., Bartkowiak-Jowsa, M., Filipiak,J.,Pezowicz,C.,Abramski,K.M., Fabrication of a polymer-based biodegradable stent using a CO2 laser. *Arch Civ Mech Eng*.,2014, **14,** 317-326. doi:https://doi.org/10.1016/j.acme.2013.08.005.

37. Gu, L., Yu, G. & Li, C. A fast and low-cost microfabrication approach for six types of thermoplastic substrates with reduced feature size and minimized bulges using sacrificial layer assisted laser engraving. *Anal. Chim. Acta*,2018, **997,** 24–34. doi:10.1016/j.aca.2017.10.030

38. Viertel, T., Pabst,L., Olbrich, M., *et al.* Generation of nano-voids inside polylactide using femtosecond laser radiation. *Appl. Phys. A, 2017,* **123,** 1–10. doi:10.1007/s0039-017-1410-7

39. Kumar, S. P. and S. Profile and depth prediction in single-pass and two-pass CO 2 laser microchanneling processes. *J. Micromechanics Microengineering*,2015,**25,**35010. doi:10.1088/0960-1317/25/3/035010

40. Prakash, S. & Kumar, S. Experimental and theoretical analysis of defocused CO_2 laser microchanneling on PMMA for enhanced surface finish. *J. Micromechanics Microengineering, 2017,* **27,** 25003. doi:10.1088/1361-6439/27/2/025003

41. Grabow, N., Schlun, M., Sternberg, K., Hakansson, N., Kramer, S., Schmitz K-P. Mechanical properties of laser cut poly(L-lactide) micro-specimens: implications for stent design, manufacture, and sterilization. J *Biomech Eng*., 2005, **127**, 25-31 doi:10.1115/1.1835349.

42. Grabow, N., Bunger,C., Shultze, C., *et al.* A biodegradable slotted tube stent based on poly(l-lactide) and poly(4-hydroxybutyrate) for rapid balloon-expansion. *Ann. Biomed. Eng.,* 2007, **35,** 2031–2038.doi:10.1007/s10439-007-9376-9

43. Chen, Y., Zhang, C., Shi, M. & Peterson, G. P. Role of surface roughness characterized by fractal geometry on laminar flow in microchannels, *Phys Rev E Stat Nonlin Soft Matter Phys*, 2009, **1,** 1–7 . doi:10.1103/PhysRevE.80.026301

44. Regehr, K. J., Domenech, M., Koepsel, J., *et al.* Biological implications of polydimethylsiloxane-based microfluidic cell culture. *Lab Chip, 2009,***9,**2132-2139. doi:10.1039/b903043c

45. Kodzius, R. *et al.* Inhibitory effect of common microfluidic materials on PCR outcome. *Sensors Actuators, B Chem.* 2012,**161,**349–358. doi:10.1016/j.snd.2011.10.044

46. Kolari, K., Satokari, R., Kataja, K., Stenman, J. & Hokkanen, A., Real-time analysis of PCR inhibition on microfluidic materials. 2008, **128,** 442–449. doi:10.1016/j.snb.2007.06.034

47. Bhattacharjee, N., Urrios, A., Kang,S, ,Folch, The Upcoming 3D-printing revolution in microfluidics, *Lab Chip*,2016,**16,**1720–1742. doi:10.1039/C6LC00163G

48. Gaal, G., Mendes, M., de Almeida, T.P., *et al.*,Simplified fabrication of integrated microfluidic devices using fusion deposition modeling 3d pinting, *Sensor and Actuators B*.2017, **242,** 35-40. doi:10.1016/j.snb.2016.10.110

50. Obaje, E. A., Cummins,G., Shilze, H., Mahmood, S., Desmulliez, M.P.Y., Bachmann,T.T. Carbon screen-printed electrodes on ceramic substrates for label-free molecular detection of antibiotic resistance. *Journal of interdisciplinary Neuromedicine.2016,***1,** 93–109. doi:10.1002/jin2.16

For Table of Content use only

Synopsis: A simple, affordable and sustainable way to prototype complex microfluidic devices using Polylactic acid, a naturally derived polymer.

TABLE OF CONTENT